

# Growth and Optical Properties of Cr<sup>3+</sup> Doped GdAlO<sub>3</sub> Single Crystals

J.P. Andreeta<sup>a</sup>, B.R. Jovanic<sup>b</sup>

*a*Instituto de Física de São Carlos, Departamento de Física e Ciência dos Materiais,  
Universidade de São Paulo, C.P. 369, 13560 São Carlos, SP, Brazil;

*b*Institute of Physics, Center of Experimental Physics, Lab.Multidisc.Res.,  
Belgrade University, P.O. Box 68, 11080 Zemun, Yugoslavia

Received: November 16, 1999; Revised: April 6, 2000

High-Temperature Solution crystal growth experiments on Cr<sup>3+</sup> doped GdAlO<sub>3</sub>, are described where the flux and solute stoichiometry was changed for the process optimization to obtain homogeneous and inclusion free larger crystals. Transparent single crystals up to 3.8 cm<sup>3</sup> have been grown. The pressure-induced wavelength shift of laser excited fluorescence in some of these crystals was measured up to 115 kbar at room temperature in relation to the R1 shift of ruby. The wavelength shift fluorescence behaviors of these doped crystals, with low Cr<sup>3+</sup> concentrations, indicate that this material could be used in producing a new class of pressure sensors.

**Keywords:** rare earth, aluminates, oxides, and high-pressure luminescence

## 1. Introduction

The rare earth aluminates are of considerable interest because of their optical and magnetic properties<sup>1-3</sup> and technological applications. The perovskite structures are strong candidates for solid state lasers as the host material for Cr<sup>3+</sup> and Nd<sup>3+</sup> in cubic and center symmetric sites, a condition necessary for obtaining long fluorescence lifetimes<sup>4</sup>. On the other hand, previous investigation on low-concentration doped Cr<sup>3+</sup> GdAlO<sub>3</sub> shows that it may be a promising material for high-pressure sensors<sup>5</sup>. The factor that restricts the technological application of the GdAlO<sub>3</sub>:Cr<sup>3+</sup> solid solutions in those systems are the inhomogeneity and the difficulties in obtaining large and high perfection single crystals. Therefore, the aim of this paper is to describe the optimized conditions to grow Cr<sup>3+</sup> doped GdAlO<sub>3</sub> crystal using the High-Temperature Solution method and to investigate the pressure-induced wavelength shift of laser excited fluorescence in some of these crystals with low doping concentrations.

## 2. Crystal Growth

### 2.1 The maximum stable growth rate criteria

Due the experimental convenience, in most of the crystal growth processes from the solution method it is usual to

adopt a linear temperature program or a constant rate of solvent evaporation. Both criteria provoke a constant flux of solute mass from liquid to solid phase. Since the crystal adsorption area will increase during crystal growth, the growth rate will be faster for small crystals, at the beginning of the crystal growth process, than for the large crystals, at the end of the process. Crystals grown under these conditions showed high concentrations of macroscopic defects near the nucleation regions due the unstable growth conditions.

Experimental results<sup>6</sup> show that the constant growth rate is also not suitable to grow large crystals due the heat and mass transport mechanism. Based in the Carlson<sup>7</sup> stability and hydrodynamics conditions, several authors [6, 8-9] found a new temperature program (Eq. 1) to grow large crystals by High Temperature Solution method known as "maximum stable growth rate":

$$T = \frac{T_0}{1 + \frac{2RT_0}{\Delta H_{\text{mix}}} \ln \left[ \cosh \left[ \frac{0.34 \beta \mu \sigma^2 C_e}{\rho_s V_{\text{sn}} P_d^{1/2} (\sigma + 1)} \right]^{1/2} t \right]} \quad (1)$$

where  $T_0$  is the initial temperature,  $\Delta H_{\text{mix}}$  is the heat of solution,  $\beta$  is the geometric crystal factor,  $\mu$  is the fluid velocity,  $\sigma$  is the relative supersaturation,  $C_e$  is the initial

<sup>a</sup>e-mail: andreeta@ifsc.sc.usp.br

equilibrium concentration,  $\rho_s$  is the solid density,  $V_{sn}$  is the initial solution volume and  $P_d$  is the Schmidt number.

### 2.2. Growth of $Cr^{3+}$ doped $GdAlO_3$

The  $Cr^{3+}$  doped  $GdAlO_3$  single crystals were grown by Czochralski, LHPG (Laser Heated Pedestal Growth) and flux methods. However, high quality large single crystals were obtained only from the flux method due the development of cracks in all the single crystals grown in the Czochralski method as shown in Fig. 1. These macroscopic defects are attributed to a structural phase transition during the cooling process at temperatures near 2073 K<sup>10</sup>. Amazingly, using LHPG method, homogeneous single crystal fibers, without cracks, with up to 0.8 mm diameter and several centimeter of length were grown, even when the annealing was performance under high temperature gradient conditions.

The high quality and homogeneous  $Cr^{3+}$  doped  $GdAlO_3$  single crystals were grown by usual flux (High-Temperature Solution) experiments carried out in sealed platinum crucibles, under the maximum stable growth rate conditions. The accelerated crucible rotation technique<sup>11</sup> was also used in some experiments in order to homogenize the liquid phase and to control the natural convection. To



**Figure 1.** Macroscopic defects (cracks) in  $Cr^{3+}$  doped  $GdAlO_3$  single crystal grown by Czochralski method.

**Table 1.**

Experimental composition (mol%)	Temperature program	Hydrodynamics conditions	Chromium concentration (mol%)	Stoichiometric deviation* (mol%)	Results and remarks
Gd <sub>2</sub> O <sub>3</sub> 8.7 Al <sub>2</sub> O <sub>3</sub> 7.5 Cr <sub>2</sub> O <sub>3</sub> 0.1 PbO 42.5 PbF <sub>2</sub> 36.1 B <sub>2</sub> O <sub>3</sub> 4.6 PbO <sub>2</sub> 0.5	Maximum stable growth rate program (Eq. 1)	Accelerated crucible rotation technique	1.7	16	Clear Crystals up to 23 x 21 x 8 mm <sup>3</sup> -Inclusions free crystals except near in the nucleations regions (unstable growth regions)

\*Deviation from the ratio Gd/Al = 1.

optimize the crystal growth experiments, several flux compositions were tried. These starting materials and the results of the main experiments are published elsewhere<sup>12</sup>. All flux compositions were based on intrinsic properties previously discussed by several authors<sup>13</sup>. The major solvent constituents have low eutectic temperature (763 K; 66 mol% of PbF<sub>2</sub>), high solubility for the crystal constituents and suitable viscosity at growth temperature that can contribute to mass transport. The additive compounds (B<sub>2</sub>O<sub>3</sub>, PbO<sub>2</sub> and V<sub>2</sub>O<sub>5</sub>) are important as oxidizing agents and to control the nucleation rate, probably by increasing the width of the metastable regions.

The best results in growing these crystals were obtained using the compositions and conditions of Table 1. From the data of this table we note that an excess of Gd<sub>2</sub>O<sub>3</sub> was added in the growth experiment (non-stoichiometric composition) to avoid a decrease in the Gd<sup>3+</sup> concentration in the solution that might lead to GdOF formation<sup>13</sup> during the crystallization process.

The experimental and theoretical temperature programs (based on the maximum stable growth rate criteria), carried out in most of crystal growth experiments, are shown in Fig. 2. The nucleation control was performed by the slow temperature fluctuation method described elsewhere<sup>14</sup>.

From the maximum stable growth rate criteria we can distinguish, in this experiment, two growth conditions: a) unstable growth, b) stable growth. The stability conditions transition occurred near 1500 K and 4,0 mm crystal size.

### 2.3. High temperature solutions crystal growth results

Using this optimized composition, associated with an appropriate temperature program and a suitable hydrodynamic condition, we could grow large and nearly homogeneous, inclusions free, single crystals. As shown in Fig. 3, the macroscopic defects could be noted only in small regions near the nucleation's point.

The  $Cr^{3+}$  doping concentration and the Pb solvent incorporation was determined by electron microprobe in

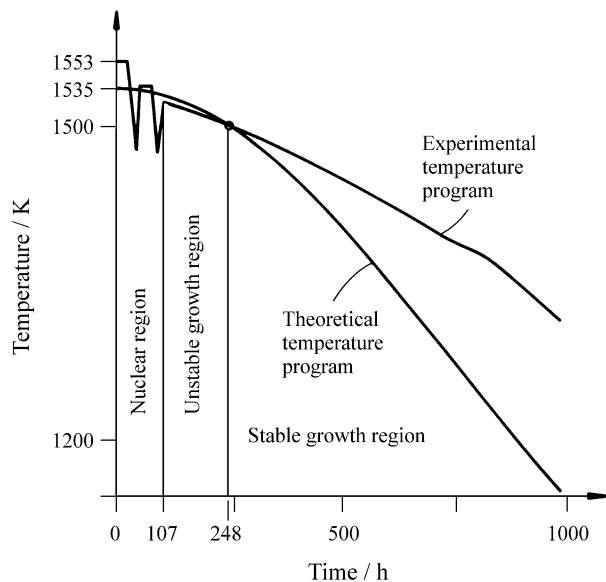


**Figure 2.** The experimental and theoretical temperature programs, based on the maximum stable growth rate criteria after<sup>8</sup>.

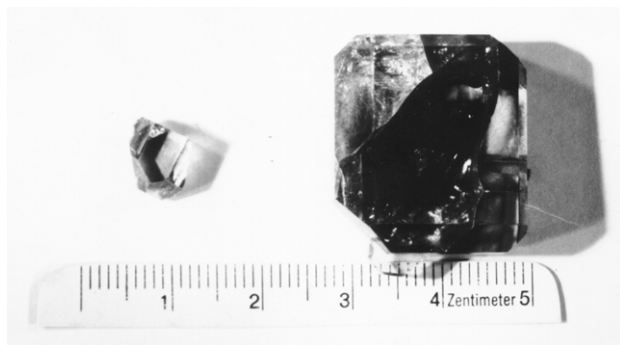


**Figure 3.** Single crystals of  $\text{GdAlO}_3:\text{Cr}^{3+}$  grown by HTS. Left - clear crystal grown after the unstable growth conditions; right - Bulk crystal showing unstable growth conditions near the nucleation regions.

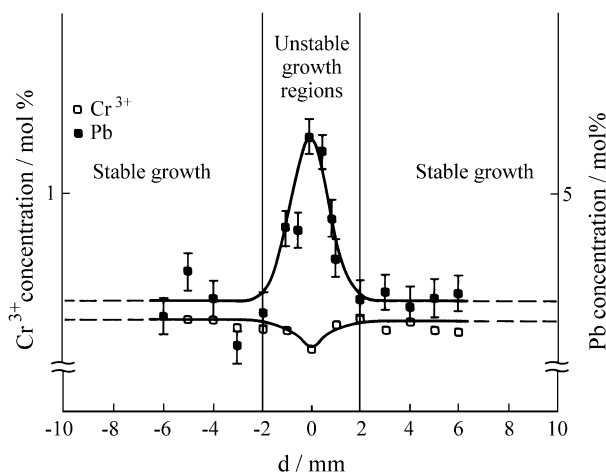


**Figure 4.**  $\text{Cr}^{3+}$  concentration and Pb incorporation profiles in the larger crystal. The distance ( $d$ ) was measured from the nucleation point.

several samples. As shown in Fig. 4, the profile for the  $\text{Cr}^{3+}$  concentration does not obey accurately the Burton, Prim and Slichter equation<sup>15</sup> for a  $k_{\text{eff}} = 0.38$ <sup>14</sup>. The  $\text{Cr}^{3+}$  distribution is nearly constant in the whole crystal, whereas the Pb incorporation has a maximum in the nucleation point probably due to unstable growth as estimated from the calculated temperature program.

### 3. Optical Properties

#### 3.1. High-pressures optical measurements

A diamond anvil cell (DAC) of the NBS type, with 1/3 carat stones, was used to generate pressure<sup>16</sup>. The pressure was increased at room temperature, and the DAC was allowed to equilibrate for at least 12 h after pressure was set up. The pressure used was in the range of 0-115 kbar and at room temperature, 300 K. A small ( $\approx 30 \mu\text{m}$ ) chip of ruby (0.1% mol  $\text{Cr}^{3+}$ ) and the  $\text{GdAlO}_3:\text{Cr}^{3+}$  (0.7% mol  $\text{Cr}^{3+}$ ) crystal were placed in the 300 $\mu\text{m}$  hole of a pre-indented stainless steel gasket, together with a methanol-ethanol (4:1) mixture that served as the pressure medium and which remained hydrostatic up to 140 kbar<sup>16</sup>. A spectrofluorometer connected with a multiscaler card in a PC was used as a measuring apparatus. The pressure was determined by the shift of the ruby R1 line (0.0365 nm/kbar)<sup>1,8</sup>. The position of the ruby R1 line and sample R line was determined using a double optical monochromator with a 0.05 nm spectral resolution and a photon counter with a multiscaler. The samples were excited by an argon ion laser at 488 nm. In order to reduce the laser heating of the sample the power of the laser was reduced to 3 mW.

#### 3.2. Results and discussion

The room-temperature emission spectra of  $\text{GdAlO}_3:\text{Cr}^{3+}$ , containing 0.7 mol% of  $\text{Cr}^{3+}$ , were obtained at two pressures; these spectra are shown in Fig. 5.

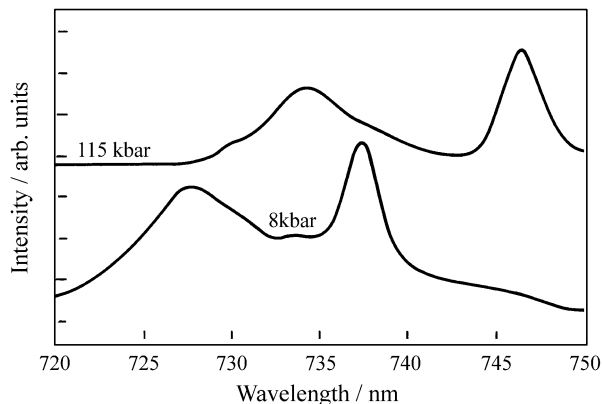


**Figure 5.** High-pressure fluorescence spectra of  $\text{GdAlO}_3:\text{Cr}^{3+}$  crystal at room temperature (0.7 mol%  $\text{Cr}^{3+}$  in the crystal).

The obtained spectrum shows only two well-resolved lines: a) the first, broad line at about 730 nm with the line width about 15.0 nm, and b) the second line is sharp or peaking at about 736 nm, with a line width of about 3.5 nm. This is contrary to the fluorescence spectra in  $\text{GdAlO}_3:\text{Cr}^{3+}$  with a 0.7 mol% concentration of  $\text{Cr}^{3+}$  at room temperature. The first line is an R line and appears to be due to transitions between the  $\text{Cr}^{3+}$  states  ${}^2\text{E}$  and  ${}^4\text{A}_2$ <sup>16</sup>. The sharp line was denoted in a previous paper as a NPL (Neighboring Pair Line)<sup>5,17</sup>. NPL is related to the energy transfer between the so-called  $\text{Cr}^{3+}$  single ions, which are nearly isolated from each other, and from the exchange coupled  $\text{Cr}^{3+}$  pairs formed statistically by  $\text{Cr}^{3+}$  ions on neighboring lattice sites.

The pressure dependence of the positions for NPL line at room temperature is presented on Fig. 6. The position of NLS line under pressure shifts linearly to the red, similar to the R line of ruby, but with larger rates 0.088 nm/kbar and 0.0364 nm/kbar, respectively. The pressure shifting rate for the NPL line is about 2.42 times larger than ruby's R line.

Similar to  $\text{GdAlO}_3:\text{Cr}^{3+}$ , several materials have luminescence line peaks far enough away from the solid-state materials broad-emission maximum:  $\text{YAlO}_3:\text{Cr}^{3+}$  with a peak at 722.80 nm<sup>20</sup>,  $\text{MgO}:\text{V}^{2+}$  at 870nm<sup>22</sup> and  $\text{YAlO}_3:\text{Nd}^{3+}$  at 875.7 nm<sup>21</sup>. All mentioned materials have a smaller pressure shift rate than the NPL line pressure shift rate for  $\text{GdAlO}_3:\text{Cr}^{3+}$ . For  $\text{YAlO}_3:\text{Cr}^{3+}$  it is 0.070 nm/kbar<sup>20</sup>, for  $\text{MgO}:\text{V}^{2+}$  is 0.055 nm/kbar<sup>22</sup>; and for  $\text{YAlO}_3:\text{Nd}^{3+}$  it is -0.014 nm/kbar<sup>21</sup>. On the other hand, some pressure sensors have a peak far away on the other side of the broad-emission maximum:  $\text{YAG}:\text{Sm}^{2+}$  at 617,7 nm<sup>23</sup>;  $\text{YAG}:\text{Eu}^{3+}$  at 590 nm<sup>25</sup>;  $\text{LaOCl}:\text{Eu}^{3+}$  at 578,7 nm<sup>24</sup>. However, their sensitivity to pressure is relatively small: for  $\text{YAG}:\text{Sm}^{2+}$  it is +0.0298 nm/kbar<sup>24</sup>; for

$\text{YAG}:\text{Eu}^{3+}$  it is 0.0197 nm/kbar<sup>25</sup>; and for  $\text{LaOCl}:\text{Eu}^{3+}$  it is 0.025 nm/kbar<sup>24</sup>.

The intensity of the NPL line is about 1.25 time larger than the intensity of the R line. Single crystals with higher  $\text{Cr}^{3+}$  ion concentration however, its intensity is approximately 0.35 smaller<sup>5</sup>. The relative intensity (background ratio) of the NPL line (0.40) is larger than for the R line in ruby (0.01),  $\text{YAlO}_3:\text{Cr}^{3+}$  (0.28) and  $\text{R}_2\text{-Z}_2$  line in  $\text{YAlO}_3:\text{Nd}^{3+}$  (22) [20] but smaller than for the R line in  $\text{MgO}$  (0.92) and  $\text{YAG}:\text{Cr}^{3+}$  (0.53) [20]. Also, the NPL line intensity change only slightly with pressure,  $\cong 4\%$ . The linewidth of the NPL line at higher pressures increases by about 20%.

## 4. Conclusions

It is possible to grow (using an appropriate solvent composition and temperature program, and a suitable hydrodynamic condition) large and nearly homogeneous  $\text{Cr}^{3+}$  doped  $\text{GdAlO}_3$  single crystals. These doped crystals, with low chromium concentrations, can be used as active elements in pressure sensors due to the large pressure shift of the NPL line; strong sharp NPL luminescence line; the relatively high fluorescence intensity that is easily detectable at pressures lower than 115 kbar and the fact the NPL peaks far away from the wavelengths of the region in which most solid-state materials doped with  $\text{Cr}^{3+}$  have maximum.

## Acknowledgments

The authors would like to acknowledge the MSTs and CNPq - Brazilian agency for financial support.

## References

1. Cashion, J.D.; Cooke, A.H.; Hawkes, J.F.P.; Leask, M.J.M.; Thorp, T.L.; Wells, M.R. *J. Appl. Phys.*, v. 39, p. 1360, 1968.
2. Cashion, J.D.; Cooke, A.H.; Leask, M.J.M.; Thorp, T.L.; Wels, M.H. *J. Mater. Sci.*, v. 3, p. 402, 1968.
3. Sivadriere, J.; Quezel-Ambrunas, S. *Compt. Rend.* (Paris), v. B 273, p. 619, 1971.
4. Murphy, J.; Olmann, R.L.; Mazelsky, R. *Phys. Rev. Letters*, v. 13, p. 135, 1964.
5. Jovanic, R. B.; Andreeta, J.P. High Pressure Effect of Fluorescence Spectra of  $\text{Cr}^{3+}$  in  $\text{GdAlO}_3$ , *J. Phys. Cond. Matt.*, v. 10 p. 271, 1998.
6. See, for example, Scheel, H.J.; Elwell, D.J. *Crystal Growth*, v. 12, p. 153, 1972.
7. Carlson, A.E. *Growth and Perfection and Crystal*, John Wiley, N.Y., p. 421, 1958.
8. Scheel, H.J.; Elwell, D. *Crystal Growth from High Temperature Solutions*, Academic Press, p. 264, 1975.

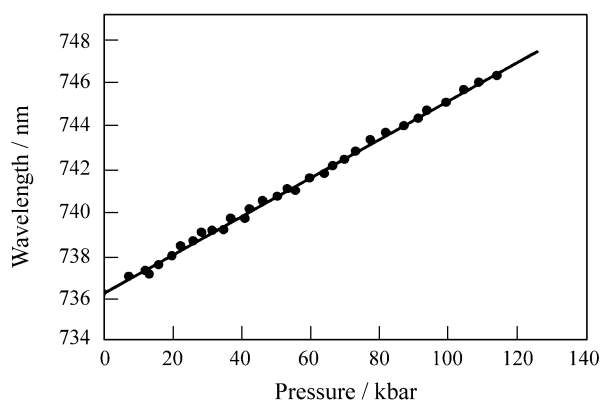


**Figure 6.** Shift in peak of fluorescence of NPL line in  $\text{GdAlO}_3$  (0.7 mol%  $\text{Cr}^{3+}$  crystal concentration) with increasing pressure at room temperature.

9. Andreeta, J.P. *Revista de Fisica Aplicada e Instrumentação*, v. 1, n. 1 p. 97, 1985.
10. Mazelsky, R.; Kramer, W.E.; Hopkins, R.H. *J. Crystal Growth* v. 2, p. 209, 1968.
11. Elwell, D.; Scheel H.J. *Crystal Growth From High Temperature Solutions*, Academic Press, London, p. 368, 1975.
12. Andreeta, J.P.; Hernandez, A.C.; Gallo, N.J.H. *Mat. Res. Bull.*, v. 25, p. 51, 1990.
13. Pamplin, B.R. *Crystal Growth*, Pergamon Press, Oxford, p. 217, 1985.
14. Andreeta, J.P.; Hernandez, A.C.; Gallo, N.J.H. *Mat. Res. Bull.*, v. 24, p. 83, 1989.
15. Burton, J.A.; Prim, H.C.; Slichter, W.P. *J. Chem. Phys.*, v. 21, p. 1987, 1953.
16. Jovanic, B.R. Lifetime of Ruby R1 Line under Ultra-high Pressure, *Chem. Phys. Lett.* v. 190, p. 440, 1992.
17. Jayaraman, A. Ultrahigh pressure *Rev. Mod. Phys.*, v. 55 p. 65, 1983.
18. Ohlmann, C.R.; Murphy, J. Exchange Interaction between Cr<sup>3+</sup> and Gd<sup>3+</sup> in GdAlO<sub>3</sub>. *Bull. Amer. Phys. Soc.*, v. 11 p. 255, 1966.
19. Jovanic, B.R. and Andreeta, J.P. GdAlO<sub>3</sub>:Cr<sup>3+</sup> as a New Pressure Sensor, *Physica Scripta*, v. 59, p. 274, 1999.
20. Barnett, J. D.; Block, S.; Piermarini, J.G. An Optical Fluorescence System for Quantitative Pressure Measurement in the Diamond, *Anvil Cell Rev. Sci. Instrum.*, v. 40 p. 1, 1973.
21. Lacam, A.; Cahteau, C. Higher-pressure measurements at moderate temperature in a diamond anvil cell with a new optical sensor: SrB<sub>4</sub>O<sub>7</sub>:Sm<sup>2+</sup>. *J. Appl. Phys.*, v. 66, p. 368, 1989.
22. Chopelas, A.; Boehler, R. *Abstract AIRAPT Conf. S'h*, SUNY, Albany, N.Y., 1983.
23. Bi, Q.; Brown, M.J.; Sato-Sorensen, Y. Calibration of Sm:YAG as an alternative high-pressure scale *J. Appl. Phys.*, v. 68 p. 5357, 1990.
24. Chi, Y.; Liu, S.; Shen, W.; Wang, L.; Zou, G. Crystal Field Analysis for Emission Spectra of LaOCI:Eu<sup>3+</sup> Under High Pressure, *Physics*, v. 139-140 p. 555, 1986.
25. Arashi, H.; Ishigama, M. Diamond Anvil Pressure Cell and Pressure Sensor for High-Temperature Use *Jap. J. Appl. Phys.*, v. 21 p. 1647, 1982.